

Near-field photocurrent imaging of the optical mode profiles of semiconductor laser diodes

T. Guenther, V. Malyarchuk, J. W. Tomm, R. Müller, and C. Lienau^{a)}

Max-Born-Institut für Nichtlineare Optik und Kurzzeitspektroskopie, Max-Born-Str. 2a, D-12489 Berlin, Germany

J. Luft

OSRAM Opto Semiconductors, Wernerwerksstr. 2, D-93049 Regensburg, Germany

(Received 30 March 2000; accepted for publication 27 November 2000)

The potential of near-field photocurrent spectroscopy for direct imaging of mode profiles of submicron-sized waveguides in optoelectronic devices is demonstrated. The technique combines the submicron spatial resolution of near-field optics with tunable laser excitation, allowing for selective investigation of the waveguide properties of the device structure. Experiments on InGaAs/AlGaAs high-power laser diodes with different waveguide designs provide direct visualization of the effect of the waveguide design on (i) the number of guided modes and (ii) the spatial profile of both fundamental and higher-order modes. The technique thus provides a sensitive tool for nondestructive *in situ* analysis of waveguide properties in optoelectronic devices. © 2001 American Institute of Physics. [DOI: 10.1063/1.1342206]

Optical waveguides are key ingredients of all semiconductor diode lasers. They confine the optical mode inside the laser cavity to dimensions in the micron or even submicron range and thus ensure sufficient overlap of the optical mode and the gain medium, e.g., a double quantum well (DQW) layer inside the waveguide. While the theoretical description of the waveguide mode structure by solving Helmholtz' equations is well established,^{1,2} it is generally quite complicated to experimentally image the optical mode structure directly. From an application point of view, such imaging is of considerable interest as it would allow to characterize the effects of waveguide imperfections^{3,4} or dopant profiles on the waveguide mode structure. This requires optical techniques with subwavelength spatial resolution, such as near-field scanning optical microscopy,^{5,6} that overcome the diffraction-limited resolution of far-field microscopy by using evanescent fields in the vicinity of nanometer-sized objects, such as apertures in metal-coated fiber probes⁶ or sharp metal tips.⁷ Information on transversal optical mode profiles of laser diodes was obtained by spatially resolved collection of the laser emission.^{8,9} These techniques are limited to those modes that contribute to the laser emission. This limitation can be overcome and the mode structure of both the fundamental and of higher waveguide modes can be imaged by monitoring the position-dependent coupling of a localized light source into these modes using the recently introduced technique of near-field photocurrent spectroscopy.^{10–12}

In this letter, we demonstrate the potential of this technique for directly mapping the optical mode profiles in waveguides by experimentally and theoretically studying near-field photocurrent images of high-power laser diodes of different waveguide designs.

In our experiments, we investigated asymmetrically coated (In)AlGaAs/GaAlAs/GaAs high-power laser diodes

with different waveguide designs. All samples consist of an active region of two 8 nm (In)AlGaAs quantum wells (DQW) inside an Al_{0.3}Ga_{0.7}As step-index (SIN) waveguide that is clad by two 1.5 μm wide Al_{0.6}Ga_{0.4}As layers. We compare structures with (i) the DQW centered inside a 440 nm wide SIN waveguide (diode A), (ii) a 1000 nm SIN waveguide (DQW symmetrically centered, diode B), and (iii) a 1000 nm SIN region with a DQW that is off-centered by 120 nm (diode C). All samples are antireflection (AR) coated with an ~120-nm-thick Al₂O₃-layer. The photon energy of the laser emission is 1.53 eV (λ = 808 nm), for all three diodes.

In the *near-field* photocurrent (NPC) experiments, the laser diode is excited by light transmitted through a 100–150 nm aperture at the end of a metal-coated near-field fiber probe.¹² The photoinduced current across the *p-i-n* junction is detected as a function of the tip position as the tip is scanned across the diode facet. Tunable continuous wave lasers are used as excitation sources and the photoinduced signal is detected with a lock-in amplifier with the laser diode unbiased.

Macroscopic *far-field* photocurrent (PC) spectra, recorded with a spatial resolution of about 500 μm, show a characteristic signal increase at an excitation energy of 1.53 eV that results from the onset of the interband absorption from the first heavy hole to the first electron subband in the DQW. The more than two orders of magnitude smaller contribution to the PC signal at energies below 1.53 eV is related to light absorption by defects inside the waveguide.¹³ The far-field PC spectra are similar for all three diodes. The excellent agreement between far-field and spatially integrated near-field PC spectra ensures that near-field scans allow to analyze the microscopic origin of far-field PC spectra.¹⁶

Two-dimensional NPC images have been recorded for the three laser structures for different excitation wavelengths. A representative image for diode A and excitation at 1.53

^{a)}Author to whom correspondence should be addressed; electronic mail: lienau@mbi-berlin.de

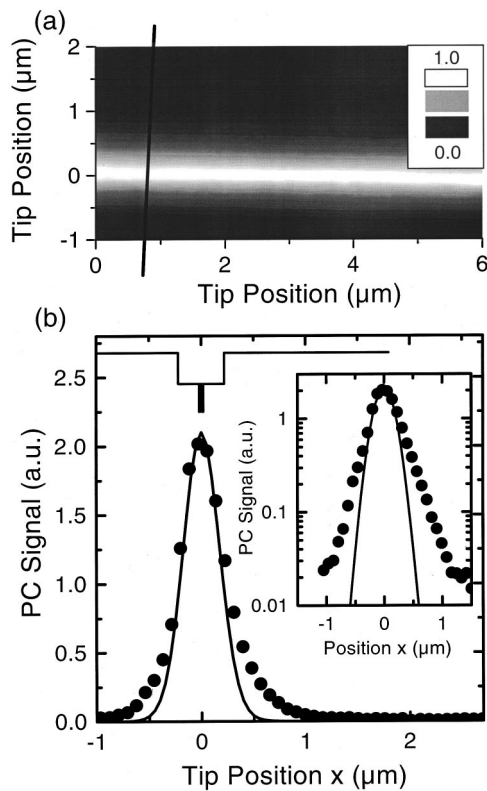


FIG. 1. (a) Two-dimensional NPC image of a laser diode with a $0.44 \mu\text{m}$ wide SIN waveguide (diode A). (b) Cross section of the NPC signal along the x axis, perpendicular to the active layer (circles: experimental, solid line: simulation). Inset: NPC signal on a logarithmic intensity scale.

eV, slightly above the onset of the DQW absorption, is shown in Fig. 1(a). All images are rather homogeneous as the tip is scanned along the y axis, parallel to the DQW layer, while pronounced spatial variations in PC signal intensity are observed along x , perpendicular to the DQW layer. Figure 1(b) shows a cross section through the two-dimensional image for diode A (440 nm wide SIN waveguide) along the x axis. In the inset the data are displayed on a logarithmic intensity scale. We observe a single narrow NPC peak with a full width at half maximum (FWHM) of 400 nm , which is centered at the DQW position. Outside the waveguide region, the signal intensity decays exponentially with increasing x [Fig. 1(b), inset]. Different NPC images are observed for diode B ($1 \mu\text{m}$ wide SIN waveguide, centered DQW) for the same excitation energy of 1.53 eV , Fig. 2. The cross section along x shows a narrow peak with a FWHM of about 250 nm centered at the DQW position. This peak is surrounded by two weaker, slightly broader and asymmetric side peaks that are separated by 400 nm from the central peak. The width of the entire triple peak structure is about $1 \mu\text{m}$, corresponding to the width of the SIN waveguide layers. For diode C ($1 \mu\text{m}$ wide SIN waveguide, off-centered DQW, Fig. 3), the triple peak is almost entirely washed out and the NPC signal consists of only a single broad peak with a width of 950 nm .

In these experiments, the light transmitted through the near-field fiber probe constitutes an excitation source of sub-wavelength dimension that is coupled into the laser waveguide. The p - i - n junction of the laser diode then serves as a local photodetector, which detects the light intensity that is

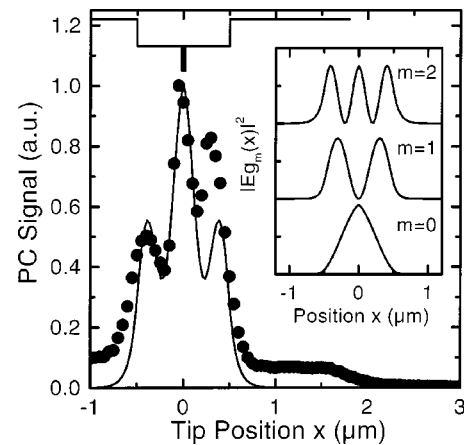


FIG. 2. NPC trace along the x axis of diode B with a $1 \mu\text{m}$ wide SIN waveguide and a centered DQW (circles: experimental, solid line: simulation). Inset: $|E_{g_m}(x)|^2$ for the three guided modes of the laser waveguide.

coupled into and absorbed within the waveguide. For metal-coated near-field aperture probes, the electromagnetic field distribution directly below the aperture consists of a superposition of both evanescent and propagating waves.¹⁴ The contribution from evanescent waves decays in the Al_2O_3 AR coating between near-field probe and diode layers. Therefore, the electric field distribution $E_{\text{in}}(x, y)$ in the plane of the antireflection/diode interface, $z=0$, that is coupled into the laser waveguide consists basically only of propagating fields with a maximum lateral component $k_{\text{lat}} = \sqrt{k_x^2 + k_y^2}$ of the wave vector $\mathbf{k} = (k_x, k_y, k_z)$ of $2\pi n_{\text{AR}}/\lambda$. Calculations of the field propagation through the multilayer structure within a matrix transfer formalism show that the corresponding spatial intensity $I_{\text{in}}(x, y) = |E_{\text{in}}(x, y)|^2$ is well described by a Gaussian profile with a FWHM of 200 nm centered at the tip position. Thus, the effective spatial resolution in the experiment is not limited by the aperture diameter but is close to the diffraction-limited resolution defined by the refractive index of the AR coating, n_{AR} . This approximation seems valid if the AR layer thickness exceeds the decay length of the evanescent field $\lambda/2\pi n_{\text{AR}}$. The efficiency for coupling $|\eta_m|^2$ into a mode m of the waveguide is then given by

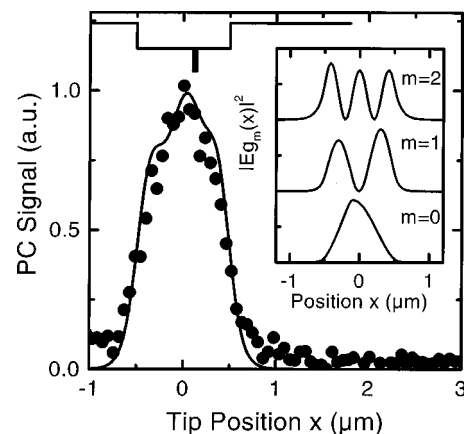


FIG. 3. As Fig. 2 for diode C with a $1 \mu\text{m}$ wide SIN waveguide and a DQW that is off-centered by 120 nm .

$$|\eta_m|^2 = \left| \int \int_{-\infty}^{\infty} E_{\text{in}}(x,y) E_m^*(x,y) dx dy \right|^2 / \left(\int \int_{-\infty}^{\infty} |E_{\text{in}}|^2 dx dy \int \int_{-\infty}^{\infty} |E_m|^2 dx dy \right), \quad (1)$$

with $E_m(x,y)$ being the electric field distribution of waveguide mode m in the plane $z=0$.¹⁵ The coupling efficiency therefore maps the square of the overlap integral of the incident electric field E_{in} and the field profile of mode m . The field distribution inside the waveguide $E_w(\mathbf{r})$ can be decomposed into a superposition of a finite number of guided modes, $Eg_{m,i}(\mathbf{r})$, and a quasicontinuum of unguided or radiation modes, $Er_{n,i}(\mathbf{r})$:

$$E_w(\mathbf{r}) = \sum_{m,i} a_{m,i} Eg_{m,i}(\mathbf{r}) + \sum_{n,i} a_{n,i} Er_{n,i}(\mathbf{r}), \quad (2)$$

where $i = \text{TE, TM}$ denotes the mode polarization. For weakly guiding optical waveguides, the spatial mode profiles for TE and TM polarization are almost identical. We therefore restrict the following discussion to $i = \text{TE}$ polarization. The mode profiles $Eg_m(\mathbf{r})$ and $Er_n(\mathbf{r})$ are obtained by solving Helmholtz' equation. We find that the waveguide of diode A supports two guided modes. The intensity profile [proportional to $|Eg_m(\mathbf{r})|^2$] of the fundamental mode $m=0$ is shown in the inset in Fig. 1. The increase in waveguide thickness from 440 nm to 1 μm in diodes B and C increases the number of bound modes to three. Intensity mode profiles are shown in the insets of Figs. 2 and 3, respectively. Note that the off-center QW position in diode C breaks the lateral symmetry of the mode profiles. The spatial structures of these profiles have typical dimensions of 0.4 μm , larger than the width of I_{in} . Therefore, the efficiency of the coupling into the respective modes depends sensitively on the position of the near-field probe within the waveguide.

To simulate the near-field images one has to evaluate the contribution of each excited waveguide mode to the PC signal. We assume that the PC signal is only generated by carrier absorption in the DQW layer. Around the laser photon energy, the far-field PC spectra vary linearly with the DQW absorption coefficient.¹⁶ Thus absorption of propagating modes m is characterized by an effective absorption coefficient $\alpha_{\text{eff},m} = -\text{Im}(k_{z,m}^2) / [2 \text{Re}(k_{z,m})]$ which is defined by the overlap integral of mode profile and DQW and the DQW absorption coefficient. Due to the presence of the AR layer the contribution of evanescent modes is negligible. The total PC signal can then be written as the superposition of the contribution from guided and radiation modes as $I_{\text{PC}} \propto \sum_m |\eta_m|^2 \alpha_{\text{eff},m} + \sum_n |\eta_n|^2 \alpha_{\text{eff},n}$. The second term, the contribution from radiation modes, gives rise to a spatially slowly varying background signal for tip positions within the waveguide and cladding layers. Our simulations and experiments show that this contribution modes is significantly smaller than that from guided propagating waveguide modes.¹⁷ The NPC images therefore map the space-dependent coupling of a localized light source into propagating guided modes of the laser waveguide and their absorption by the active DQW layer.

For active layers positioned in the center of the waveguide only modes of even symmetry are effectively absorbed, with a typical absorption length of about 10 μm .

Therefore, for diode A only the ground mode $m=0$ contributes to the NPC signal. The width and overall shape of the experimental NPC trace are well reproduced (Fig. 1). A closer inspection shows that the experimentally observed exponential decay of the signal for excitation outside the waveguide is weaker than the calculated one. This decay length is a sensitive measure of the difference in refractive indices between waveguide and cladding layers.^{1,2} This difference is obviously overestimated in our simulations that did not consider the effect of doping on the refractive indices of the core/cladding layer.

As the number of guided modes is increased by changing the waveguide width to 1 μm , the NPC signal of diode B shows a superposition of $m=0$ and $m=2$ modes. Its overall shape is again well reproduced. Not reproduced is the pronounced asymmetry of the experimental trace. Such an asymmetry may only be obtained in our simulations by assuming slightly different refractive indices in the p - and n -doped cladding layers. An off-center position of the active DQW layer (diode C) induces absorption of all three bound modes, $m=0-m=2$. Consequently, the pronounced triple peak structure observed for diode B is almost entirely washed out, as observed experimentally and theoretically (Fig. 3).

In conclusion, we have presented near-field photocurrent study of high-power laser diodes of different waveguide structures. We have experimentally and theoretically demonstrated the potential of this technique for directly imaging the mode profiles of optical waveguide structures of submicron dimensions.

¹D. Marcuse, *Theory of Dielectric Optical Waveguides* (Academic, London, 1974).

²A. W. Snyder and J. D. Love, *Optical Waveguide Theory* (Chapman and Hall, London, 1983).

³A. G. Choo, H. E. Jackson, U. Thiel, G. N. de Brabander, and J. T. Boyd, *Appl. Phys. Lett.* **65**, 947 (1994).

⁴S. Z. Bourzeix, J. M. Moison, F. Mignard, F. Barthe, A. C. Boccara, C. Licoppe, B. Mersali, M. Allovon, and A. Bruno, *Appl. Phys. Lett.* **73**, 1035 (1998).

⁵D. W. Pohl, W. Denk, and M. Lanz, *Appl. Phys. Lett.* **44**, 651 (1984).

⁶E. Betzig, J. K. Trautman, T. D. Harris, J. S. Weiner, and R. L. Kostelak, *Science* **251**, 1468 (1991).

⁷E. J. Sanchez, L. Novotny, and X. Sunney Xie, *Phys. Rev. Lett.* **82**, 4014 (1999).

⁸C. Lienau, A. Richter, A. Klehr, and T. Elsaesser, *Appl. Phys. Lett.* **69**, 2471 (1996).

⁹I. Horsch, R. Kusche, O. Marti, B. Weigl, and K. J. Ebeling, *J. Appl. Phys.* **79**, 3831 (1996).

¹⁰S. K. Buratto, J. W. P. Hsu, E. Betzig, J. K. Trautman, R. B. Bylisma, C. C. Bahr, and M. J. Cardillo, *Appl. Phys. Lett.* **65**, 2654 (1994).

¹¹M. S. Unlu, B. B. Goldberg, W. D. Herzog, D. Sun, and E. Towe, *Appl. Phys. Lett.* **67**, 1862 (1995).

¹²A. Richter, J. W. Tomm, C. Lienau, and J. Luft, *Appl. Phys. Lett.* **69**, 3981 (1996).

¹³J. W. Tomm, A. Jaeger, A. Bärwolff, T. Elsaesser, A. Gerhard, and J. Donecker, *Appl. Phys. Lett.* **71**, 2233 (1997).

¹⁴R. D. Grober, T. Rutherford, and T. D. Harris, *Appl. Opt.* **35**, 3488 (1996).

¹⁵K. J. Ebeling, *Integrated Optoelectronics* (Springer, Berlin, 1993).

¹⁶J. W. Tomm, T. Günther, Ch. Lienau, A. Gerhardt, and J. Donecker, *J. Cryst. Growth* **210**, 296 (2000).

¹⁷The contribution from radiation modes is expected to become significant if the thickness d_z of the waveguide structure (600 μm in our diodes) is much shorter than $1/\alpha_{\text{eff},m}$ ($\sim 10 \mu\text{m}$). In such thin waveguides, the propagating mode contribution reduces linearly with d_z and becomes less dominant as d_z approaches the wavelength of the light.